Magnetic moments and magnetic site susceptibilities in Mn_5Si_3

2002 J. Phys.: Condens. Matter 14 8707

(http://iopscience.iop.org/0953-8984/14/37/307)

INSTITUTE OF PHYSICS PUBLISHING JOURNAL OF PHYSICS: CONDENSED MATTER

J. Phys.: Condens. Matter **14** (2002) 8707–8713 PII: S0953-8984(02)36762-6

Magnetic moments and magnetic site susceptibilities in Mn_5Si_3

M Ramos Silva[1], P J Brown[2] and J B Forsyth[3]

[1] CEMDRX, Departamento de Física, Universidade de Coimbra, 5004-516 Coimbra, Portugal
[2] Institut Max von Laue-Paul Langevin, BP 156X, 38042 Grenoble Cedex, France
[3] Rutherford Appleton Laboratory, Chilton, Oxon OX11 0QX, UK

E-mail: brown@ill.fr

Received 9 May 2002
Published 5 September 2002
Online at stacks.iop.org/JPhysCM/14/8707

Abstract

Polarized neutron diffraction has been used to determine the manganese magnetic moments aligned by magnetic fields applied parallel to the [001] axis in the antiferromagnetic phases of Mn_5Si_3. It has been found that in the two antiferromagnetic phases which exist below T_N the magnetic moments on the manganese sites which can be aligned by a magnetic field all have the same order of magnitude, although in the antiferromagnetic structures the ordered moments are very different. The transition, on cooling, from the AF2 to the AF1 phase is accompanied by a sharp decrease in the susceptibilities of all the sites. This uniform decrease is not consistent with disordered local moments on the sites which do not have ordered moments, but can be understood using the same criteria for stability of Mn moments as have been invoked for manganese rare-earth compounds (Ballou R, Lacroix C and Nunez Regueiro M D 1991 *Phys. Rev. Lett.* **66** 1910).

1. Introduction

Mn_5Si_3 is the prototype phase with the $D8_8$ structure; the unit cell is hexagonal with space group $P6_3/mcm$ [2]. The manganese atoms are located in two different crystallographic sites. Full crystallographic details are given in table 1.

The magnetic structure of Mn_5Si_3 has been studied by [4] using neutron diffraction on single crystals. These show the existence of two antiferromagnetic phases named AF2 and AF1. AF2 is stable between the Néel temperature at 99 and 66 K, at which temperature it undergoes a first-order transition to the second antiferromagnetic phase AF1. With the onset of long-range magnetic order the symmetry is reduced to orthorhombic. The orthorhombic cell dimensions at 70 K are $a_o = 6.898\,56(1)$, $b_o = 11.9120(2)$ and $c_o = 4.793\,30(1)$ Å [5] and these are related to those of the hexagonal cell by $a_o \approx a_h$, $b_o \approx \sqrt{3}a_h$, $c_o \approx c_h$. The orthorhombic cell is face centred, space group $Ccmm$, with $Z = 4$. In this space group, as indicated in table 2 and

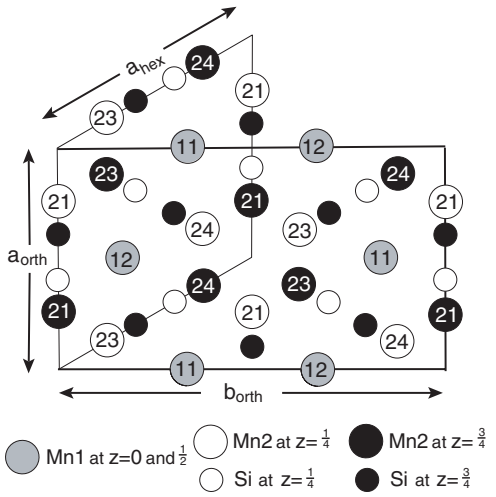

Figure 1. Projection down [001] of the orthorhombic unit cell of Mn_5Si_3 showing the relationship between the orthorhombic and hexagonal unit cells. The Mn23 and Mn24 sites together are the Mn22 sites of the AF2 phase.

Table 1. Crystallographic data for Mn_5Si_3.

Space group: $P6_3/mcm$; $Z = 2$ Unit cell: $a = 6.910$, $c = 4.814$ Å at 300 K			
Atomic positions			Site symmetry
4 Mn1 in 4(d)	1/3, 2/3, 0		32
6 Mn2 in 6(g)	x_1, 0, 1/4	$x_1 = 0.2360$[a]	mm
6 Si in 6(g)	x_2, 0, 1/4	$x_2 = 0.5991$[a]	mm

[a] Parameters from [3].

Table 2. Manganese positions in the two antiferromagnetic phases of Mn_5Si_3.

AF2 phase									
Atomic positions and site symmetry			Space group		Atomic positions and site symmetry			Space group	
			$Cmcm$[a]	$Ccmm$[b]				$Ama2$[a]	$Cc2m$[b]
8 Mn1	8(e)	2	x_0, 0, 0	0, x_0, 0	Mn11	4(a)	2	0, 0, z_{11}	0, z_{11}, 0
					Mn12	4(a)	2	0, 0, z_{12}	0, z_{12}, 0
4 Mn21	4(c)	mm	0, y_{21}, $\frac{1}{4}$	y_{21}, 0, $\frac{1}{4}$	4 Mn21	4(b)	m	$\frac{1}{4}$, y_{21}, z_{21}	y_{21}, z_{21}, $\frac{1}{4}$
4 Mn22	8(g)	m	x_{22}, y_{22}, $\frac{1}{4}$	y_{22}, x_{22}, $\frac{1}{4}$	Mn23	4(b)	m	$\frac{1}{4}$, y_{23}, z_{23}	y_{23}, z_{23}, $\frac{1}{4}$
					Mn24	4(b)	m	$t\frac{1}{4}$, y_{24}, z_{24}	y_{24}, z_{24}, $\frac{3}{4}$
$x_0 \approx z_{11} \approx 1/3$					$z_{12} \approx 2/3$				
$y_{21} \approx x_1$					$z_{21} \approx 0$				
$x_{22} \approx y_{22} \approx y_{23} \approx z_{23} \approx x_1/2$					$y_{24} \approx z_{24} \approx 1 - x_1/2$				

[a] Space group with standard setting: $Cmcm$, number 63; $Ama2$, number 40.
[b] Space group with axes oriented such that $a_o \approx a_h$, $b_o \approx \sqrt{3}a_h$, $c_o \approx c_h$.

illustrated in figure 1, the 12 Mn2 sites divide into two independent sets; 4 Mn21 atoms occupy 4(c) positions with site symmetry mm and the remaining 8 Mn22 atoms (Mn23 and Mn24 in

the AF1 phase: see below) are in 8(g) positions with site symmetry m. Magnetic reflections indexed on this cell have $h+k$ odd corresponding to the magnetic propagation vector 010. The magnetic structures of both the AF2 and AF1 phases have been established using single-crystal neutron diffraction and zero-field neutron polarimetry [5, 6]. In the AF2 structure the Mn1 and the Mn21 atoms have no ordered moment whilst the Mn22 atoms have a moment of 1.48(1) μ_B directed parallel and antiparallel to b. Below 66 K, the magnetic moments re-align and adopt a highly non-collinear magnetic structure (AF1 phase). In this structure, the moments are in general directions. Although the magnetic structure has monoclinic magnetic symmetry the atomic positions can still be described with orthorhombic symmetry, although in a non-centrosymmetric space group (table 2). The Mn22 sites (Mn23 and Mn24) (figure 1) related by the centre of symmetry are no longer magnetically equivalent. At 4.2 K the Mn1 atoms (Mn11 $\approx$ Mn12) have moments of $\mu = 1.20(5)$ μ_B and are oriented parallel and antiparallel to the direction with polar coordinates $\theta = 116(1)^\circ$, $\phi = 105(1)^\circ$, where θ is measured from [001] and ϕ from (010). The Mn21 atoms again carry no moment, whilst for Mn23 $\theta = 70(1)^\circ$, $\phi = 93(1)^\circ$, $\mu = 2.30(9)$ μ_B and for Mn24 $\theta = 21(1)^\circ$, $\phi = 11(7)^\circ$ and $\mu = 1.85(9)$ μ_B.

These magnetic structures, in which magnetic atoms with the same chemical environment have very different magnetic moments, are somewhat unusual although rather similar situations occur in some manganese–rare-earth alloys [7]. The present experiment exploits the sensitivity of polarized neutron scattering to determine the site susceptibilities of the magnetically distinct manganese atoms in Mn_5Si_3. The results can be used to determine to what extent the topological frustration in the structure leads to collapse of the Mn moments as in $TbMn_2$ [8] or whether the low moments observed in the antiferromagnetic structures are simply due to lack of complete alignment of local Mn moments.

2. Experimental details

Polarized neutron diffraction provides a sensitive method of measuring the magnetic scattering associated with magnetic moments aligned parallel to an external magnetic field. In the series of experiments described below, the polarization dependence of the peak intensity scattered by selected Bragg reflections (flipping ratio measurements) was measured. The data were collected with the polarized neutron diffractometer D3 which receives neutrons from the hot source of the ILL nuclear reactor. The sample was mounted in the variable-temperature insert of an asymmetric split-coil superconducting magnet which can give a magnetic field up to a maximum of 4.6 T parallel to the ω-axis of the diffractometer. The samples used in the experiments were cut from a large (1 g) single crystal of Mn_5Si_3 kindly supplied by the late Dr Menshikov of the Institut for Metal Physics, Ekaterinburg. The sample used for the polarized neutron measurements had linear dimensions $\approx$5 mm and a smaller $\approx$3 mm sample was used for the structural work.

2.1. Unpolarized neutron diffraction

In order to deduce the magnetic structure factors from polarized neutron flipping ratios it is necessary to have a good knowledge of both the nuclear structure and the degree of extinction exhibited by the crystal. For this reason a set of integrated intensity measurements was made on the four-circle diffractometer D9 which is equipped with a small-area detector. The sample used was the smaller of the two crystals described above. The intensities of 151 reflections with $\sin\theta/\lambda < 0.5$ Å^{-1} were measured at 60 K. After averaging over equivalents, these yielded 29 independent structure factors with an internal agreement factor between equivalent reflections, after averaging, of $R(F^2) = 0.01$.

2.2. Equi-domain samples

In a preliminary experiment the field dependence of the intensity of a $\{0\frac{1}{2}0\}$ reflection, which is characteristic of the AF1 phase and is absent in the AF2 phase, was measured. It was established that at 58 K its intensity dropped sharply between 2.8 and 4 T applied along [001]: showing that at this temperature the transition takes place within the range of fields (1–4.6 T) in which polarized neutron flipping ratios can be measured on D3. The polarized neutron flipping ratios of 18 $hk0$ reflections were then measured at fields of 3.6 and 4.6 T. At lower fields 1, 2.6 and 3.4 T a smaller set containing only six reflections was selected. At each field the value of the integrated intensities of the antiferromagnetic reflections $\{\frac{1}{2}00\}$, $\{\frac{1}{2}20\}$, $\{\frac{1}{2}\bar{2}0\}$ were measured to monitor the transition from the AF1 to the AF2 phase. A further set of measurements was made at 63 K in which the flipping ratios of the 100, 110 and 220 reflections were measured at 1, 2, 3 and 4.6 T.

2.3. Sample with unequal domains

A crystal which is cooled through the Néel temperature without external constraints is expected to contain three different orthohexagonal domains with roughly equal populations. In such a crystal each nuclear Bragg reflection contains contributions from the aligned magnetic moments in all three domains, and their sum has the hexagonal symmetry of the nuclear structure. For an equi-domain crystal it is therefore only possible to distinguish between the crystallographically distinct Mn1 and Mn2 sites and not between the subsets of Mn2 atoms. However, the magnetic moments in the AF2 phase are oriented parallel to the orthorhombic b-axis and it is therefore expected that the three domains will have different energies in a field applied in the ab-plane. To test this hypothesis the crystal was mounted with an orthorhombic a-axis parallel to the field and cooled through the Néel temperature in 4.6 T. Subsequent measurement of the integrated intensities of equivalent antiferromagnetic reflections from different orthohexagonal domains confirmed that a large difference in the population of these domains had been induced. However, to compare the site susceptibilities, the field must be applied along the [001] axis. For this experiment therefore, the crystal was mounted in a special device to allow an *in situ* 90° rotation of the vertical axis after field cooling. The crystal was fixed inside a cylindrical container which was able to rotate about its axis. The hexagonal [120] axis (orthorhombic [010]) was parallel to the rotation axis which was horizontal. The [001] direction was also initially horizontal but the activation of a spring forced a 90° rotation, changing the vertical axis from [100] to [001]. Using this device the crystal was cooled with the orthorhombic a-axis (hexagonal [100]) parallel to the applied magnetic field of 4.6 T and then rotated so that the c-axis was vertical. Analysis of the integrated intensities of the magnetic reflections gave domain populations of 0.550(2), 0.226(2) and 0.224(2). The polarized neutron flipping ratios of a series of $hk0$ reflections were then measured at 80 K with the magnetic field remaining at 4.6 T.

3. Analysis of the results

3.1. Nuclear structure factors

The structure refinement was performed using the least-squares program SFLSQ [9]. Atomic positions, isotropic thermal displacement parameters and an extinction correction were refined. After the first cycles the isotropic extinction parameter refined to zero and was then kept constant. The refinement converged to the residual $R(F) = 0.013$ and $\chi^2 = 8.2$. The final values of the refined parameters are given in table 3.

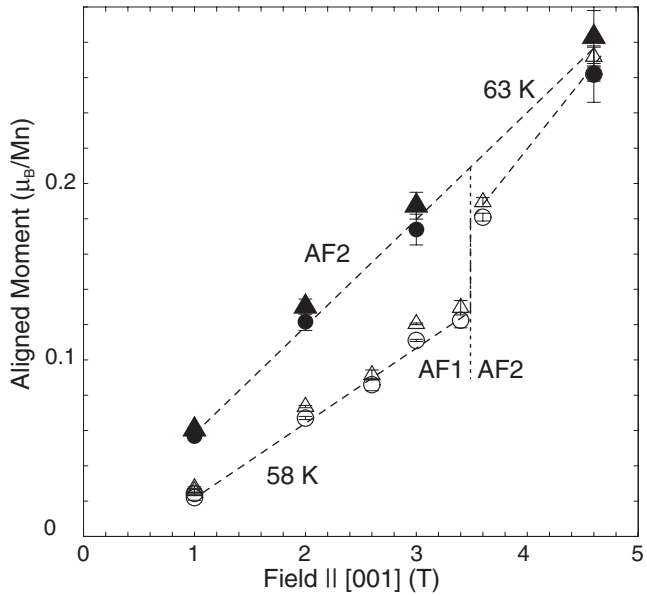

Figure 2. Evolution of the ferromagnetically aligned moments in Mn_5Si_3 with applied field. The open and solid symbols correspond to measurements made at 63 and 58 K, respectively. The triangles and circles give results for the Mn1 and Mn2 sites respectively.

Table 3. Parameters obtained in the refinement of the low-temperature magnetic structure of Mn_5Si_3.

	Mn1	Mn2	Si
x-parameter	—	0.2361(3)	0.5994(2)
Isotropic temperature factor (Å^{-2})	0.13(6)	0.12(7)	0.25(7)

3.2. Determination of the site susceptibilities

Magnetic structure factors were calculated from the flipping ratios using nuclear structure factors obtained using the structure parameters of the unpolarized neutron refinement. The usual corrections, including those for incomplete beam polarization, were applied to the data. These magnetic structure factors were used to determine the components of the moments aligned parallel to the field at the Mn sites of the structure.

The data measured as a function of applied field in the experiment with the magnetic domains equally populated were used to determine the magnetic moments on the two distinct manganese (Mn1, Mn2) sites using a least-squares fitting procedure. The residual values for the fits for each magnetic field range from 4.2 to 12.8%. The induced moments obtained are shown in figure 2.

The data collected in the experiment with an unbalanced domain population could be analysed so as to yield the aligned components of the moments on the three sites Mn1, Mn21 and Mn22. The results obtained from a least-squares fit to the flipping ratios were: Mn1 0.1835(23) μ_B, Mn21 0.1664(29) μ_B and Mn22 0.1803(20) μ_B. The final residual factor was $R = 8.3\%$. The moments aligned on Mn1 and Mn22 are equal within the experimental error and that on Mn21 is only slightly less.

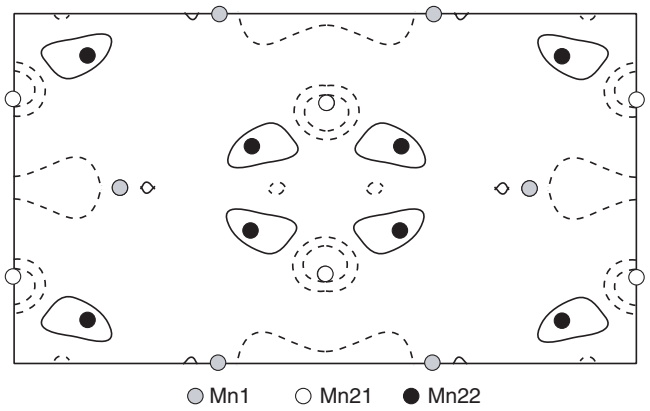

Figure 3. Projection down [001] of the maximum entropy reconstruction of the orthorhombic distortion of the aligned magnetic moment distribution of Mn_5Si_3 in 4.6 T applied parallel to [001]. Contours are drawn at intervals of 0.01 μ_B Å^{-2}.

In order to examine the difference between the Mn21 and Mn22 sites more critically, the intensities of the orthorhombic reflections that would be equivalent under hexagonal symmetry were averaged. The difference between each reflection and the corresponding hexagonal average was then calculated and these differences were used to calculate the projection down [001] of the deviation from hexagonal symmetry of the aligned magnetization, using the maximum entropy algorithm [10]. This algorithm provides the least noisy magnetization map compatible with the measured data within its error bars. The method is particularly suitable when only sparse and noisy data are available. The calculation was performed over a grid of 64×64 and the prior density was taken to be zero. The map obtained is shown in figure 3.

4. Discussion

Figure 2 shows that the susceptibilities of the Mn1 and Mn2 sites are very similar. At 63 K and 1 T the sample is already in the AF2 phase and the aligned magnetization is nearly linearly dependent on the applied field. At 58 K and 1 T, on the other hand, the AF1 phase is stable. The magnetization increases linearly with applied field, but with a smaller slope, until, at around 3.5 T, there is a sharp break corresponding to the field-induced transition from AF1 to AF2. The observation that in the transformation from AF2 to AF1 the susceptibility of both sites is reduced by the same amount is somewhat surprising as only the Mn1 sites order in this transition. If there were disordered local moments on the Mn21 sites, the susceptibility of the Mn2 sites should not change in the transition.

The stability of a magnetic moment on manganese atoms in a variety of intermetallic compounds, as evinced by the observation of an ordered moment and its magnitude, has been shown to be strongly dependent on its local environment [11]. The presence of one or more close Mn neighbours can lower the moment or, below a critical distance, suppress it entirely [12]. It has been recognized that frustration or the lack of an internal field at the Mn site can also lead to collapse of the moment [1]. A striking example of the former effect occurs at the AF2–AF1 transition in Mn_5Si_3 at which the appearance of an ordered moment on the Mn1 site in the AF1 phase is accompanied by a discontinuous expansion in the c-dimension which lengthens the two short Mn1–Mn1 bonds (Mn1–Mn1 $= c/2 = 2.41$ Å). The Mn2–Mn2 distances are in the range 2.8–2.9 Å for which a moment is expected to be stable; however, frustration at the Mn21 site could lead to its collapse.

The most significant features of the maximum entropy map of the orthorhombic distortion of the magnetization are the negative regions around the Mn21 sites. These confirm the results of the least-squares analysis which associated a smaller aligned moment with Mn21 than with the hexagonally equivalent Mn22 sites. This low susceptibility suggests that the moments on Mn atoms at these sites may indeed be close to instability, and that this instability is brought on by magnetic frustration. If the Mn2 moments are on the verge of instability it could explain the break in the Mn2 susceptibility at the AF2–AF1 transition. The aligned Mn21 moment would then be due only to the presence of the local field produced by aligned moments on neighbouring magnetic atoms, rather than to the direct effect of the applied field on a local Mn21 moment. Its diminution when the Mn1 sites order can then be understood. Similar behaviour has been found in the Laves phase Fe_2Ti [13].

5. Conclusion

Values have been obtained for the moments aligned on the Mn1, Mn21 and Mn22 sites of Mn_5Si_3 at 58 and 63 K by magnetic fields between 1 and 5 T. At each field and temperature the moments are very similar to one another. The susceptibility of all sites in the lower-temperature phase AF1 is significantly lower than that in the AF2 phase. It is possible to understand the results using the same criteria for stability of Mn moments that have been invoked for manganese rare-earth compounds.

References

[1] Ballou R, Lacroix C and Nunez Regueiro M D 1991 *Phys. Rev. Lett.* **66** 1910
[2] Aronsson B 1960 *Acta Chem. Scand.* **14** 1414
[3] Lander G H and Brown P J 1967 *Phil. Mag.* **16** 521
[4] Menshikov A Z, Vokhmyanin A P and Dorofeev Yu A 1990 *Phys. Status Solidi* b **158** 319
[5] Brown P J and Forsyth J B 1995 *J. Phys.: Condens. Matter* **7** 7619
[6] Brown P J, Forsyth J B, Nunez V and Tasset F 1992 *J. Phys.: Condens. Matter* **4** 10 025
[7] Ballou R, Deportes J, Lemaire R and Ouladdiaf B 1992 *J. Phys.: Condens. Matter* **4** 1103
[8] Brown P J, Ouladdiaf B, Ballou R and Deportes J 1988 *J. Appl. Phys.* **63** 3487
[9] Brown P J and Matthewman J C 1993 Cambridge crystallography subroutine library—mark3 *Rutherford Appleton Laboratory Report* 93-009
[10] Gull S F and Daniell G J 1978 *Nature* **272** 686
[11] Forsyth J B and Brown P J 1990 *J. Phys.: Condens. Matter* **2** 2713
[12] Wada H, Nakamura H, Yoshimura K, Shiga M and Nakamura Y 1987 *J. Magn. Magn. Mater.* **70** 134
[13] Brown P J, Deportes J and Ouladdiaf B 1992 *J. Phys.: Condens. Matter* **4** 10 015